Temporal dynamics of Prochlorococcus ecotypes in the Atlantic and Pacific oceans

Title

Temporal Dynamics of *Prochlorococcus* Ecotypes in the Atlantic and Pacific Oceans

Authors

Rex R. Malmstrom[1], Allison Coe[1], Gregory C. Kettler[1], Adam C. Martiny[1,2], Jorge Frias-Lopez[1,3], Erik R. Zinser[1,4], and Sallie W. Chisholm[1,*].

1) Department of Civil and Environmental Engineering, Massachusetts Institute of Technology, Cambridge, MA, 02139.
2) Departments of Earth System Science and Ecology and Evolutionary Biology, University of California, Irvine, CA 92693
3) The Forsyth Institute, Boston, MA, 02115
4) Department of Microbiology, University of Tennessee, Knoxville, TN, 37996
* Corresponding author

Running Title: Temporal Dynamics of *Prochlorococcus*

Subject Category: Microbial population and community ecology

Keywords: *Prochlorococcus/Synechococcus*/ecotype/time-series/HOT/BATS

Abstract

To better understand the temporal and spatial dynamics of *Prochlorococcus* populations, and how these populations co-vary with the physical environment, we followed monthly changes in the abundance of five ecotypes – two high-light adapted and three low-light adapted - over a five-year period in coordination with the Bermuda Atlantic Time Series (BATS) and Hawaii Ocean Time-series (HOT) programs. Ecotype abundance displayed weak seasonal fluctuations at HOT and strong seasonal fluctuations at BATS. Furthermore, stable 'layered' depth distributions, where different *Prochlorococcus* ecotypes reached maximum abundance at different depths, were maintained consistently for five years at HOT. Layered distributions were also observed at BATS, although winter deep mixing events disrupted these patterns each year and produced large variations in ecotype abundance. Interestingly, the layered ecotype distributions were regularly reestablished each year after deep mixing subsided at BATS. In addition, *Prochlorococcus* ecotypes each responded differently to the strong seasonal changes in light, temperature, and mixing at BATS, resulting in a reproducible annual succession of ecotype blooms. Patterns of ecotype abundance, in combination with physiological assays of cultured isolates, confirmed that the low-light adapted eNATL could be distinguished from other low-light adapted ecotypes based on its ability to withstand temporary exposure to high intensity light, a characteristic stress of the surface mixed layer. Finally, total *Prochlorococcus* and *Synechococcus* dynamics were compared with similar time series data collected a decade earlier at each location. The two data sets were remarkably similar - testimony to the resilience of these complex dynamic systems on decadal time scales.

Introduction

A key challenge facing marine microbiology is to understand how microbial diversity and biogeochemical cycles are linked, and to eventually incorporate this understanding into conceptual and predictive ocean models. Physiological and genetic analyses of cultured isolates, as well as metagenomic studies of whole communities (DeLong et al. 2006; Venter et al. 2004), are uncovering more and more about the metabolic potential of microbes comprising these assemblages. In addition, time series studies are revealing how the composition of microbial communities varies over both time and space (Carlson et al. 2009; Fuhrman et al. 2006; Treusch et al. 2009). Coupling the spatial and temporal dynamics of specific microbial groups with insights into their metabolic potential is essential for developing a quantitative understanding of the roles these microbes play in marine ecosystems.

Over the past twenty years, investigations of the unicellular cyanobacterium *Prochlorococcus* have provided insight into both the biogeography and metabolic potential of this group. *Prochlorococcus* is typically the most abundant photoautotroph in tropical and subtropical waters (Campbell et al. 1994; Partensky et al. 1999), and its abundance varies seasonally at some locations (Campbell et al. 1997; DuRand et al. 2001). Studies of cultured isolates have revealed the optimal light and temperature levels differ among the strains (Moore and Chisholm 1999; Moore et al. 2002; Moore et al. 1998; Zinser et al. 2007), as do the nutrient pools available to them (Moore et al. 2005; Moore et al. 2002). Genomic analyses of isolates (Coleman et al. 2006; Kettler et al. 2007; Rocap et al. 2003), and metagenomic analyses of natural communities (DeLong et al. 2006; Martiny et al. 2006; Martiny et al. 2009a), have provided additional insights into

the genetic diversity, metabolic potential, and evolutionary history of the group. The ability to examine the abundance and distribution of *Prochlorococcus* in the wild, and measure its genomic and metabolic properties in the lab and field, make *Prochlorococcus* a model system for advancing our understanding the ecology of marine microbes.

Prochlorococcus is composed of several clades that are physiologically and phylogenetically distinct with respect to their optimal light and temperature environments (Johnson et al. 2006; Kettler et al. 2007; Moore and Chisholm 1999; Moore et al. 1998; Rocap et al. 2002; Zinser et al. 2007). These clades have been referred to as 'ecotypes' (Moore and Chisholm 1999; Moore et al. 1998; Rocap et al. 2002) following the broader historical designation for genetically distinct subgroups within a species that are adapted to specific environments (Clausen et al. 1940; Turesson 1922). They do not necessarily conform to the more recent and narrowly-defined 'ecotype' concept developed by Cohan and others (Cohen 2001; Cohan and Perry 2007), which has become a notable model for exploring the theoretical basis for divergence among bacteria (Fraser et al. 2009, Ward et al. 2006). A more detailed discussion of the different uses of the term 'ecotype' is provided by Coleman and Chisholm (2007).

The abundance of *Prochlorococcus* ecotypes in various oceanic regions has been studied extensively (Ahlgren et al. 2006; Bouman et al. 2006; Johnson et al. 2006; West and Scanlan 1999; Zinser et al. 2006; Zinser et al. 2007). Members of the two high-light adapted (HL) ecotypes, eMIT9312 and eMED4, are most abundant in the upper regions of the euphotic zone, whereas low-light adapted (LL) ecotypes such as eNATL and eMIT9313 are most abundant in the lower euphotic zone (Johnson et al. 2006; West et al. 2001; Zinser et al. 2007). These distribution patterns agree well with differences in the

optimal light levels for representative ecotype strains (Moore and Chisholm 1999; Zinser et al. 2007). Furthermore, eMED4 tends to dominate in cooler, higher latitude waters, while eMIT9312 dominates warmer, lower latitude waters (Johnson et al. 2006; Zwirglmaier et al. 2007); also in good agreement with temperature optima of representative strains. Water column stability and nutrient concentrations have also been correlated with ecotype abundance (Bouman et al. 2006; Johnson et al. 2006), and community structure (Martiny et al. 2009b), although the underlying causalities of these relationships are not well understood.

The environmental factors influencing *Prochlorococcus* ecotype abundance, such as light, temperature, and water column mixing, vary over time and can display seasonal patterns, thus we might expect ecotype dynamics to do the same. While we have analyzed ecotype variability over span of a few days (Zinser et al. 2007), extensive time-series studies have not been conducted, and thus little is known about the dynamics of *Prochlorococcus* ecotypes on the scale of months to years. Analyses on these time scales should help refine our understanding of ecotype/environment interactions, and provide datasets for testing models designed to explore the dynamics of phytoplankton community structure (Follows et al. 2007).

To this end, we followed the spatial and temporal dynamics of *Prochlorococcus* ecotypes at monthly intervals over five years in coordination with the Bermuda Atlantic Time Series (BATS) and the Hawaii Ocean Time-series (HOT) programs (Karl and Lukas 1996; Steinberg et al. 2001). Both programs are focused on oligotrophic, open ocean sites where *Prochlorococcus* is found in abundance (Campbell et al. 1994; DuRand et al. 2001). However, the physics and chemistry of these locations differ, most notably

by the stronger seasonal mixing events at BATS and the higher inorganic phosphate concentrations at HOT (Cavender-Bares et al. 2001; Steinberg et al. 2001; Wu et al. 2000). Here we explore how changes in environmental factors such as mixing, light, and temperature are related to ecotype abundance and distribution, as well as how they co-vary temporally over 5 years. We also examine some of the emergent patterns in the field data through studies of light-shock tolerance in cultured isolates of different *Prochlorococcus* ecotypes.

Methods and Methods

Sample Collection

Beginning in November 2002, flow cytometry and qPCR samples were collected over a five-year period during monthly cruises for the Bermuda Atlantic Time Series (BATS) and Hawaii Ocean Time-series (HOT) programs. Additional samples were collected bi-weekly between February and April at BATS. Samples were collected from twelve depths (1, 10, 20, 40, 60, 80, 100, 120, 140, 160, 180, and 200m) at the BATS site (~5 nautical mile radius around 31° 40'N, 64° 10' W), and from twelve depths (5, 25, 45, 60, 75, 85, 100, 115, 125, 150, 175, and 200m) at Sta. ALOHA (~5 nautical mile radius around 22° 45'N, 158° 00'W). These locations are referred to BATS and HOT throughout the manuscript for simplicity.

Flow Cytometry

Whole seawater samples were immediately fixed with glutaraldehyde (final conc. 0.125% v/v) for 10 minutes, frozen in liquid nitrogen, and stored at –80°C until samples

could be processed in the laboratory using an Influx flow cytometer (Becton Dickinson). *Prochlorococcus* and *Synechococcus* populations were identified and quantified based on their unique autofluorescence and scatter signals (Olson et al. 1990a; Olson et al. 1990b). *Prochlorococcus* could not always be clearly distinguished in the upper 40m at BATS from June-September, thus these profiles were excluded from depth-integrated counts in Figure 2. Flow cytometry profiles from early 2003 were not processed.

Primer Re-design for Ecotype eSS120

New primers for the eSS120 ecotype were designed in ARB (Ludwig et al. 2004), using a large database of environmental ITS sequences (Martiny et al. 2009b). These primers, 5'-AAC AAA CTT TCT CCT GGG CT-3' and 5'-AGT TGA TCA GTG GAG GTA AG-3', matched 87% of known eSS120 ITS sequences, but did not target MIT9211. The specificity of the primers was initially tested against cultured isolates from other ecotypes such as MIT9313, MIT9312, MED4, and NATL2a. These tests confirmed specificity within the dynamic range of the assay (~5 to 5 X 10^5 cells mL^{-1}). Specificity was also confirmed by cloning and sequencing ITS regions amplified from field samples from BATS and HOT using the new primers. All amplified ITS sequences clustered with strains SS120 and MIT9211, both members of the eSS120 ecotype (Kettler et al. 2007), in a boot-strapped (n=100) neighbor-joining tree constructed with the Bosque software package (Ramirez-Flandes and Ulloa 2008) (Supp. Fig. 1). The new primers substantially increased counts of the SS120 ecotype (Supp. materials).

Quantitative PCR

Samples for qPCR were collected and processed as described previously (Ahlgren et al. 2006; Zinser et al. 2006; Zinser et al. 2007) with two small modifications. First, reaction volumes were reduced from 25µL to 15µL and performed in 384-well plates on the Light Cycler 480 for samples collected after 2003. Second, concentrations of eMIT9313-specific primers were increased to 5 µM to improve sensitivity. Estimated abundances that fell below the lowest value of the standard curve were set to the theoretical detection limit of 0.65 cells mL^{-1}. Samples were excluded if their melt curves contained multiple peaks or peaks different from those in the DNA standards to ensure only the targeted ecotypes were quantified. Missing data were determined by linear interpolation when abundance estimates were available for the depths immediately above and below the missing value.

Environmental Data Extraction

Temperature, salinity, and potential density were downloaded from the HOT and BATS websites. Missing data were determined by linear interpolation when values were available for the depths immediately above and below the missing data point. Mixed layer depths, light attenuation coefficients, and *Prochlorococcus* and *Synechococcus* abundance (1991-1995) were also downloaded directly from the HOT website. Mixed layer depths and attenuation coefficients at BATS were calculated from bottle-derived profiles and SeaWiFS Profiling Multichannel Radiometer profiles of photosynthetically active radiation (PAR) collected by Bermuda Bio-Optics Program. The mixed layer depth was determined when potential density differed from surface values by > 0.125 kg

m^{-3}. Attenuation coefficients at BATS were calculated by linear regression of log-transformed PAR values; only profiles with an $R^2 > 0.993$ were used.

Solar Irradiance

Surface irradiance was determined from SeaWiFS-derived estimates of daily-integrated PAR. Eight-day means of daily integrated PAR values from March 2000 to July 2006 were calculated from a 27km by 27km region around BATS and HOT (White et al. 2007). A two component Fourier model with a period of 1 year was fitted to PAR data, producing an R^2 of 0.90 and 0.93 at BATS and HOT, respectively. Modeled PAR data were used to estimate surface irradiance on the day of sample collection. This model was necessary to account for seasonal variability in solar flux due to changes in day length and solar azimuth. These changes result in a roughly two-fold difference in daily-integrated solar flux between summer and winter (e.g. ~20,000 – 56,000 mE m^{-2} d^{-1} at BATS, and ~31,000 – 58,000 mE m^{-2} d^{-1} at HOT, using this model).

The relationships between ecotype abundance and PAR plotted in Figure 1 and Supplementary Figure 2 were determined using robust locally weighted linear regression (LOWESS) in MATLAB. Robust LOWESS is more resistant to outliers (Cleveland 1979), which are defined in MATLAB's robust LOWESS function as data outside six mean absolute deviations.

Time Series and Other Statistical Analyses

Integrated ecotype abundance, surface PAR, and mixed layer depth were log-transformed, detrended, and resampled at a regular monthly interval to meet the

mathematical requirements for time series analyses (Legendre and Legendre 1998). Detrended data were calculated as the residuals of linear regression of log-transformed data against time. Detrended data were resampled every 30.44 days, which is equivalent to twelve measurements per year, using linear interpolation. Coefficients of autocorrelation and cross-correlation were determined in MATLAB, and standard deviations calculated as $n^{-1/2}$, where n is the number or resampled data points. Spectral analysis by discrete Fourier transformation, calculated using the Fast Fourier Transformation (FFT) algorithm, was also performed in MATLAB. The power spectral density was estimated as the absolute value of FFT^2.

Differences among ecotypes in the average depth of maximum abundance were tested using repeated-measures ANOVA, followed by a Tukey post-test (α=0.05), using MATLAB.

Non-parametric partial correlation coefficients (Spearman R) were calculated in MATLAB to determine the relationship between abundance and temperature while controlling for the influence of light.

Light Shock Experiments

Serial batch cultures of axenic *Prochlorococcus* strains MED4, NATL2a, and SS120 were grown in Sargasso seawater-based Pro99 media (Moore et al. 2007) and illuminated by cool white fluorescent lamps. Cultures were transferred at least four times to acclimate them to 35 μE m^{-2} s^{-1} of continuous light. Duplicate acclimated cultures that were in log-phase growth were then exposed to 400 μE m^{-2} s^{-1} for four hours before being returned to their initial light levels. *In vivo* chlorophyll fluorescence was measured

before and after light shock with a 10-AU fluorometer (340-500 nm excitation and 680 nm emission filters), and cell counts determined by flow cytometry as described above.

Results and Discussion

Ecotype distribution with light and temperature

Striking similarities between HOT and BATS emerged when data from all depths and all 5 years were combined for a synoptic analysis of *Prochlorococcus* ecotype abundance along irradiance/depth gradients (Fig. 1 a,b ; Supp. Fig. 2). As expected, the two high-light adapted ecotypes, eMIT9312 and eMED4, were most abundant at higher irradiances, with abundance dropping off sharply below 1,500 mE m^{-2} d^{-1} of photosynthetically-active radiation (Fig. 1a,b; Supp. Fig. 2a,e). In contrast, two low-light adapted ecotypes, eSS120 and eMIT9313, usually reached maximum abundances between 100-250 mE m^{-2} d^{-1}, and were typically at or near detection limits at irradiances >1,500 mE m^{-2} d^{-1}. The eNATL group, also low-light adapted, had an intermediate distribution, reaching maximum abundance at 300-600 mE m^{-2} d^{-1}. Unlike the other low light ecotypes, eNATL abundance was occasionally high at irradiance levels >1,500 mE m^{-2} d^{-1} (Fig. 1a,b; Supp. Fig. 2c,h), which is consistent with hypothesis that eNATL can tolerate exposure to higher light levels than eSS120 and eMIT9313 (Coleman and Chisholm 2007; Zinser et al. 2007).

This consistent relationship between irradiance and ecotype abundance results in a 'layered' depth distribution at both locations (Fig. 1a-d). At HOT, for example, HL ecotype eMIT9312 tended to reach maximum abundance at shallower depths than did its fellow HL ecotype eMED4 (Table 1). LL ecotypes also partitioned the water column at

HOT, with eNATL abundance peaking at significantly shallower depths than eSS120 and eMIT9313 (Table 1). Similar patterns in ecotype distribution were also observed at BATS (Table 1; Fig. 1b,d), except for during deep mixing events, defined here as when the mixed layer depth was >100m. During periods of deep mixing physical homogenization appears to overwhelm biological partitioning of the water column, resulting in uniform depth distributions (Fig. 1e,f). Therefore, data from periods of deep mixing were removed from statistical analysis of depth distributions.

It is remarkable that, with the exception of periods of deep mixing, the general patterns of ecotype abundance appear relatively consistent in the Atlantic and Pacific despite substantial differences in the chemical and physical environment. Furthermore, these patterns are consistent with those found previously in a variety of ocean regions (Bouman et al. 2006; Johnson et al. 2006; West and Scanlan 1999; West et al. 2001; Zinser et al. 2006; Zinser et al. 2007). That is, the ecotypes tend to partition the water column by depth, with eNATL reaching maximum abundance in between the peaks of HL ecotypes MED4 and MIT9312, and other LL ecotypes. The similarities in the distributions along depth/light gradients suggest that *Prochlorococcus* ecotypes are responding in a consistent fashion to irradiance regardless of geography.

Temporal Dynamics: Depth-integrated Prochlorococcus and Synechococcus populations

Using flow cytometry, we measured the abundance of *Prochlorococcus*, and its close relative *Synechococcus* (Rocap et al., 2002), to provide an overall framework for exploring *Prochlorococcus* ecotype dynamics. At BATS, the depth-integrated

Prochlorococcus population displayed a strong seasonal pattern, reaching the highest levels in the late summer and fall, and the lowest in the late winter during the annual deep mixing events (Fig. 2a). *Synechococcus* displayed the inverse pattern, and even occasionally exceeded the abundance of *Prochlorococcus* during deep mixing events (Fig. 2b). This is the same pattern reported by DuRand et al. (2001) for *Prochlorococcus* and *Synechococcus* at BATS from 1990-1994 (Fig. 2a,b). The concordance between these two data sets is remarkable, given that they are separated by more than a decade.

Variations in *Prochlorococcus* and *Synechococcus* abundance were much less dramatic at HOT. Integrated abundance of *Prochlorococcus* varied just over 2-fold throughout the time series, and did not always reach maximal abundance in the summer or minimal abundance in the winter (Fig 2c). *Synechococcus* still displayed an annual pattern, tending to reach peak abundance during winter, but they were never as abundant as *Prochlorococcus*, in contrast to what was observed at BATS. These abundance and variability levels are also consistent with those observed over a decade ago at HOT (Fig. 2c,d)

Temporal Dynamics: Depth-integrated ecotype abundance patterns

As was seen in the total *Prochlorococcus* population, the depth-integrated (0-200m) abundance of all five ecotypes followed clear annual patterns at BATS (Fig. 3a). Spectral analysis of each ecotype revealed dominant peaks in the power spectrum at a period of one year (Supp. Fig. 3), and autocorrelations displayed a sinusoidal pattern, with peaks in autocorrelation every twelve months (Supp. Fig. 4). Furthermore, fitting a single component Fourier series with a period of 1 year to each ecotype produced R^2

values ranging from 0.48 (eMIT9313) to 0.67 (eSS120), indicating that most of the variability in integrated abundance could be accounted for by an annual oscillation.

Annual variations in temperature and mixed layer depth were smaller at HOT than at BATS, as were the variations in ecotype abundance (Fig. 3b). While spectral analysis did reveal that all ecotypes had a peak in the power spectrum at a period of 1 year, this was not the only strong signal, particularly for the LL ecotypes (Supp. Fig. 5). Fitting a single component Fourier series with a period of 1 year to each ecotype produced R^2 values ranging from only 0.17 (eMIT9312) to 0.33 (eMIT9313). In addition, autocorrelations did not display the same strong sinusoidal pattern as seen at BATS (compare Supp. Fig. 3 with Supp. Fig. 6). Thus, while there was a component of annual variability to ecotype abundance at HOT, there was also variability at periods greater and less than one year. This suggests that when annual environmental variations are more moderate, the impact of intra- and inter-annual events, such as passage of mesoscale eddies or El Niño/La Niña oscillations - both known to influence primary production and phytoplankton community composition at HOT (Bibby et al. 2008; Corno et al. 2007; Karl et al. 1995; Letelier et al. 2000) - may become more pronounced.

Although ecotype abundance followed a clear annual cycle at BATS, the cycles were not synchronized among ecotypes, i.e. different ecotypes reached peak abundance at different times. In each of the five years, the eNATL ecotype reached its maximum integrated abundance about four months after winter deep mixing events (Table 2), typically in June (Supp. Fig. 7). Abundance of eMED4 peaked roughly one month later, while the LL-clades eSS120 and eMIT9313 reached maximal abundance about eight months after the deep mixing event (Table 2). HL ecotype eMIT9312 also reached

maximal abundances at around the same time as eSS120 and eMIT9313, typically in October or November (Supp. Fig. 7). The regularity of this pattern indicates that each ecotype responded to changes in environmental conditions in different, yet consistent ways, resulting in an annually repeating succession of ecotypes.

The succession of *Prochlorococcus* ecotypes is in some ways reminiscent of classical phytoplankton succession models, although it is occurring at a much smaller phylogenetic scale; all *Prochlorococcus* differ in 16S rRNA sequence by <3% (Moore et al. 1998), which would collectively constitute a single bacterial species by conventional standards (Stackebrandt and Goebel 1994). Interestingly, two recent time series studies at BATS have also uncovered annual cycles and succession patterns in other microbial groups, most notably the SAR11 clade (Carlson et al. 2009; Treusch et al. 2009). For example, one SAR11 subgroup reaches peak abundance in surface waters during the summer, while another subgroup peaks in the winter (Carlson et al. 2009). SAR11 bacteria are the most abundant heterotrophs at BATS and are major consumers of dissolve organic compounds (Malmstrom et al. 2005; Morris et al. 2002), whereas *Prochlorococcus* is the most abundant photoautotroph and a substantial source of dissolved organics (Bertilsson et al. 2005; DuRand et al. 2001). In addition, SAR11 bacteria and *Prochlorococcus* are both major consumers of small compounds like amino acids and dimethylsulfoniopropionate (DMSP) (Malmstrom et al. 2004; Michelou et al. 2007; Vila-Costa et al. 2006; Zubkov et al. 2003), which are significant sources of C,N, and S to marine microbial communities. Therefore, it seems plausible that succession in these two abundant groups could be linked through the production of, and competition

for, dissolved organic compounds. Uncovering potential links in the dynamics of the dominant microbial groups presents a future challenge.

Ecotype abundance in different regions of the euphotic zone

Variations in light and temperature levels, which impact the growth of *Prochlorococcus* (Johnson et al. 2006; Moore and Chisholm 1999; Zinser et al. 2007), are greater in surface waters than at depth. Thus integrating abundance across the entire water column likely obscures important features in ecotype dynamics. To get a more detailed understanding of the temporal and spatial dynamics of the ecotypes, we analyzed integrated abundance in three sections of the euphotic zone (0-60m, 60-120m, and 120-200m).

The HL-adapted ecotype eMIT9312 displayed similar abundance patterns in the upper (0-60m) and middle (60-120m) euphotic zone at BATS, but below 120m the seasonal cycle was out of phase with surface cycles by several months (Fig. 4a; Fig. 5a). Abundance in the lower euphotic was positively correlated with mixed layer depth (Spearman $R = 0.5$; $p < 0.05$), and abundance peaks occurred simultaneously with annual deep mixing events (Fig. 4a). This suggests that it is the transport of surface populations below 120m, and not *in situ* growth, that may be responsible for most of the annual variation in abundance of eMIT9312 in the lower euphotic zone at BATS.

As with eMIT9312, patterns of eMED4 abundance in the upper and middle euphotic zone also differed from those in the lower zone at BATS (Fig. 5b), with strong spikes in abundance below 120m accompanying deep mixing (Fig. 4b). But while the eMED4 and eMIT9312 dynamics were synchronized below 120m, these HL-adapted

ecotypes were out of synchronization by several months in the upper 120m (Fig. 5a,b). That is, each year at BATS, eMED4 typically reached peak abundance in July-August, whereas eMIT9312 reached maximum abundance in October-November (Supp. Fig. 7). At HOT, in contrast, these two HL ecotypes did not display these offset repeating patterns.

We hypothesize that different temperature sensitivities of eMED4 and eMIT9312 explain, at least in part, the differences in their temporal dynamics at BATS. That is, strains belonging to the eMED4 clade have lower temperature optima than those belonging to the eMIT9312 clade (Johnson et al. 2006; Zinser et al. 2007). If this differential trait is universal among cells belonging to the eMED4 and eMIT9313 clades, then this would allow eMED4 cells to accumulate during the first half of the year when temperatures were low, while the higher temperature optimum of eMIT9312 would limit their accumulation until later in the season when temperatures were high – as was observed at BATS. In fact, the abundance of eMED4 in the upper 60m was negatively correlated with temperature when light levels were taken into account (partial correlation coeff. -0.43; $p<0.05$), whereas eMIT9312 abundance was positively correlated with temperature (partial correlation coeff. 0.30; $p<0.05$). The potential influence of temperature on the temporal distribution of HL ecotypes at BATS is analogous to its inferred influence on their geographic distribution: eMED4 dominates in cooler, higher latitude waters, and eMIT9312 dominates warmer, lower latitude waters (Johnson et al. 2006; Zwirglmaier et al. 2007).

Abundance patterns of eNATL also differed among regions of the euphotic zone, and the similarity of these patterns between BATS and HOT was striking. At both

locations, abundance in the upper 60m typically peaked 3-4 months earlier than at 60-120m and 120-200m (Fig. 4c,h; Fig. 5c,h). Integrated abundance in the upper 60m reached maximum levels during deep mixing events, and decreased as the mixed layer depth shoaled (Fig 4c,h). This suggests that annual peaks in abundance in the upper 60m were due, at least in part, to vertical transport of deeper cells to surface waters via mixing. While it remains unclear if members of the LL-adapted eNATL clade were able to grow at high light levels found in the upper euphotic zone, the net accumulation eNATL cells throughout the water column during periods of deep mixing confirmed that the eNATL clade was able to at least tolerate temporary exposure to high irradiance.

In contrast to eNATL, the abundance of the other two LL-adapted ecotypes, eSS120 and eMIT9313, did not increase dramatically in the upper 60m during periods of deep mixing. In fact, their abundance of was typically near or below detection levels throughout the entire water column at BATS when the well-mixed layer spanned the euphotic zone (Fig 4d,e). It appears that, unlike eNATL, members of the eSS120 and eMIT9313 ecotypes could not tolerate temporary high light exposure when transported to surface waters via mixing. At HOT, however, the mixed layer depth rarely exceeded 100m, and therefore a substantial fraction eSS120 and eMIT9313 cells were not transported to surface waters during winter mixing events. Thus, it appears that eSS120 and eMIT9313 maintained relatively stable abundance levels throughout the time series, in comparison with BATS, as they were not subjected to inhibitory, or lethal, high light exposure during mixing events.

Response to light shock in cultured isolates

To directly test the hypothesis that members of the eNATL clade can withstand temporary exposure to high intensity light better than members of the other LL-ecotypes, we performed light shock experiments with cultured isolates from the eMED4, eNATL, and eSS120 clades. Strains acclimated to an irradiance of 35 μE m^{-2} s^{-1} were exposed to light levels of 400 μE m^{-2} s^{-1} for 4 hours and then returned back to 35 μE m^{-2} s^{-1}. For perspective, these light levels are equivalent to those that would be found at 90m and 36m at mid-day, assuming a surface irradiance of 2,000 μE m^{-2} s^{-1} and an attenuation coefficient of –0.045 m^{-1}, which are typical of HOT and BATS. Furthermore, 400 μE m^{-2} s^{-1} is a lethal intensity for NATL2a and SS120, but not MED4, when applied continuously (Moore and Chisholm 1999).

In vivo chlorophyll fluorescence of all three cultures dropped significantly relative to the control after the light shock. Fluorescence in MED4 and NATL2a cultures rebounded within 24 hours and continued to increase over the next 48 hours (Fig. 6), while fluorescence of the SS120 culture continued to decline for the following 72 hours. Cell concentrations of MED4 and NATL2a also rose following the light shock, whereas the number of SS120 cells declined throughout the recovery period (Supp. Fig. 8). These results indicate that NATL2a can withstand temporary light shock better than SS120, which is consistent with the temporal and spatial distribution patterns of their respective ecotypes at HOT and BATS described above. These results are also consistent with a similar light shock experiment comparing isolates SS120 and PCC 9511, a member of the HL-adapted eMED4 ecotype. In this study, the capacity to repair damage to photosystem II caused by light shock was much greater in PCC 9511 than in SS120 (Six et al. 2009).

Although it was not tested specifically, it is plausible that NATL2a is also better able to reverse photoinactivation of photosystem II than SS120. If so, then this would present a possible mechanism to explain, at least in part, the differences in temporary light shock tolerance and the subsequent environmental distributions of LL ecotypes.

Analysis of the genomes of cultured isolates provides some insight into the genes that may be responsible for differences in light physiology among LL-adapted ecotypes. For example, the two sequenced eNATL isolates each have 41 genes encoding high light-inducible proteins (HLIPs), whereas the other LL-adapted ecotypes only have 9 to 13 HLIP genes (Coleman and Chisholm 2007). This protein family, also called small cab-like proteins, aids in high-light survival and photoacclimation in *Synechocystis* (Havaux et al. 2003; He et al. 2001), and may also play role in light-shock tolerance in eNATL. The mechanism by which they do this remains unclear, but HLIPs are thought to physically associate with either photosystem and allow it to shed excess energy as heat and thereby reduce photoinactivation (Promnares et al. 2006; Yao et al. 2007). As a photosynthetic organism, reducing and reversing the effects of photosystem inactivation is crucial for the survival of *Prochlorococcus* exposed to high light levels.

Differences in their ability to repair UV-damaged DNA of may also partially explain differences in the environmental distributions of eNATL and other LL ecotypes. The six sequenced isolates from the two HL-adapted ecotypes and the two sequenced isolates from the eNATL ecotype contain genes that encode photolyase (Coleman and Chisholm 2007; Kettler et al. 2007), an enzyme helps repair UV-damaged DNA (Sancar 2000). Photolyase genes are absent in the genomes of the other four LL-adapted isolates that have been sequenced. While these other LL-adapted isolates do encode for an

alternate putative UV-repair enzyme, pyrimidine dimer glycosylase (Goosen and Moolenaar 2008; Partensky and Garczarek 2010), its function in *Prochlorococcus* has not been confirmed. This enzyme also has a modification of the Arg-26 residue that is known to dramatically reduce activity in homologs (Doi et al. 1992; Goosen and Moolenaar 2008), suggesting a diminished ability to repair UV-damaged DNA in eSS120 and eMIT9313 ecotypes. Indeed, the high-light adapted strain MED4, which encodes photolyase, has a greater tolerance to UV exposure than low-light adapted strain MIT9313 (Osburne et al. 2010), which lacks photolyase but encodes pyrimidine dimmer glycosylase. Thus, the protection from UV exposure provided by photolyase may explain, at least in part, why the eNATL clade can better survive transport to UV-rich surface waters."

Conclusions

Clear patterns in the temporal and spatial distribution of *Prochlorococcus* ecotypes emerge from this study. For example, ecotype abundance follows a strong annual pattern at BATS, whereas ecotype abundance has only a weak annual pattern at HOT. In addition, ecotypes at BATS follow an annual succession pattern, but a similar pattern is not observed at HOT. These patterns are consistent with what we have learned from physiological assays on cultured isolates with regards to the light optima, temperature optima, and light-shock tolerance of different ecotypes. That is, the distinct distribution patterns at both HOT and BATS can be explained, at least in general terms, by the consistent and predictable responses of ecotypes to changes in the light, temperature, and mixing at each location.

Analyses of inorganic nutrient concentrations and ecotype abundance were not possible as nutrient levels were below detection in the upper 100m at BATS throughout most of this study. However, while nutrients undoubtedly influence growth rates and standing stocks of *Prochlorococcus*, their influence on specific ecotypes may not be apparent, as evidenced by the fact that general patterns can be explained without them. Indeed, recent work suggests that nitrate concentrations might impact the composition of *Prochlorococcus* populations at finer phylogenetic levels than the ecotypes examined in our study (Martiny et al 2009b). Exploring how, and at which temporal, spatial, and phylogenetic scales, chemical and biological environment influence *Prochlorococcus* abundance and diversity presents a future challenge.

Results from this study help set the stage for coupling patterns in temporal and spatial dynamics of ecotypes with insights into their metabolic potential. The next step is to understand how *Prochlorococcus* ecotypes, or even sub-groups within these ecotypes, might differ in terms of nutrient usage, dissolved organic matter production and consumption, and other metabolic processes. This understanding will come from additional studies involving strain isolation, metagenomic comparisons, and large-scale single-cell genomics.

Acknowledgements

We thank Michael Lomas and the BATS team for sample collection at Bermuda, and David Karl, Matthew Church, and the HOT team for sample collection at Hawaii. We also thank Angel White and Ricardo Letelier for assistance with deriving solar flux data and attenuation coefficients. Norm Nelson and David Court generously provided light data from the Bermuda Bio Optics Program. This work was funded by grants from the National Science Foundation, NSF STC Center for Microbial Oceanography: Research and Education, and the Gordon and Betty Moore Foundation.

References

Ahlgren, N. A., G. Rocap, and S. W. Chisholm. 2006. Measurement of *Prochlorococcus* ecotypes using real-time polymerase chain reaction reveals different abundances of genotypes with similar light physiologies. Environ. Microbiol. **8:** 441-454.

Bertilsson, S., O. Berglund, M. J. Pullin, and S. W. Chisholm. 2005. Release of dissolved organic matter by *Prochlorococcus*. Vie Et Milieu-Life and Environment **55:** 225-231.

Bibby, T. S., M. Y. Gorbunov, K. W. Wyman, and P. G. Falkowski. 2008. Photosynthetic community responses to upwelling in mesoscale eddies in the subtropical North Atlantic and Pacific Oceans. Deep-Sea Res. Part II-Top. Stud. Oceanogr. **55:** 1310-1320.

Bouman, H. A. and others 2006. Oceanographic basis of the global surface distribution of *Prochlorococcus* ecotypes. Science **312:** 918-921.

Campbell, L., H. B. Liu, H. A. Nolla, and D. Vaulot. 1997. Annual variability of phytoplankton and bacteria in the subtropical North Pacific Ocean at Station ALOHA during the 1991-1994 ENSO event. Deep-Sea Res. Part I-Oceanogr. Res. Pap. **44:** 167-&.

Campbell, L., H. A. Nolla, and D. Vaulot. 1994. The Importance of *Prochlorococcus* to Community Structure in the Central North Pacific-Ocean. Limnol. Oceanogr. **39:** 954-961.

Carlson, C. A., R. Morris, R. Parsons, A. H. Treusch, S. J. Giovannoni, and K. Vergin. 2009. Seasonal dynamics of SAR11 populations in the euphotic and mesopelagic zones of the northwestern Sargasso Sea. Isme Journal **3:** 283-295.

Cavender-Bares, K. K., D. M. Karl, and S. W. Chisholm. 2001. Nutrient gradients in the western North Atlantic Ocean: Relationship to microbial community structure and comparison to patterns in the Pacific Ocean. Deep-Sea Res. Part I-Oceanogr. Res. Pap. **48:** 2373-2395.

Clausen, J., Keck, D.D., and W.M. Hiesey. 1940. Experimental studies on the nature of species. I. Effects of varied environments on western North American plants. Carnegie Institute of Washington. **520**.

Cleveland, W. S. 1979. Robust Locally Weighted Regression and Smoothing Scatterplots. Journal of the American Statistical Association **74:** 829-836.

Coleman, M. L., and S. W. Chisholm. 2007. Code and context: *Prochlorococcus* as a model for cross-scale biology. Trends in Microbiology **15:** 398-407.

Coleman, M. L. and others 2006. Genomic islands and the ecology and evolution of *Prochlorococcus*. Science **311:** 1768-1770.

Cohan, F.M. 2001. Bacterial species and speciation. Systematic Biology **50(4):** 513-524.

Cohan, F.M. and E.B. Perry. 2007. A systematics for discovering the fundamental units of bacterial diversity. Current Biology **17(10):** R373-R386.

Corno, G. and others 2007. Impact of climate forcing on ecosystem processes in the North Pacific Subtropical Gyre. Journal of Geophysical Research-Oceans **112**.

Doi, T. and others. 1992. The role of the basic amino acid cluster and Glu-23 in pyrimidine dimer glycosylase activity of T4-endonuclease-V. Proceedings of the National Academy of Sciences of the United States of America **89 (20):** 9420-9424.

DeLong, E. F. and others 2006. Community genomics among stratified microbial assemblages in the ocean's interior. Science **311:** 496-503.

DuRand, M. D., R. J. Olson, and S. W. Chisholm. 2001. Phytoplankton population dynamics at the Bermuda Atlantic Time-series station in the Sargasso Sea. Deep-Sea Res. Part II-Top. Stud. Oceanogr. **48:** 1983-2003.

Frasier, C., Alm, E.J., Polz, M.F., Spratt, B.G., and W.P. Hanage. 2009. The bacterial species challenge: making sense of genetic and ecological diversity. Science **323:** 741-746.

Follows, M. J., S. Dutkiewicz, S. Grant, and S. W. Chisholm. 2007. Emergent biogeography of microbial communities in a model ocean. Science **315:** 1843-1846.

Fuhrman, J. A., I. Hewson, M. S. Schwalbach, J. A. Steele, M. V. Brown, and S. Naeem. 2006. Annually reoccurring bacterial communities are predictable from ocean conditions. Proceedings of the National Academy of Sciences of the United States of America **103:** 13104-13109.

Goosen, N., Moolenaar, G.F. 2008. Repair of UV damage in bacteria. DNA Repair **7 (3):** 353-379.

Havaux, M., G. Guedeney, Q. F. He, and A. R. Grossman. 2003. Elimination of high-light-inducible polypeptides related to eukaryotic chlorophyll a/b-binding proteins results in aberrant photoacclimation in Synechocystis PCC6803. Biochimica Et Biophysica Acta-Bioenergetics **1557:** 21-33.

He, Q. F., N. Dolganov, O. Bjorkman, and A. R. Grossman. 2001. The high light-inducible polypeptides in Synechocystis PCC6803 - Expression and function in high light. Journal of Biological Chemistry **276:** 306-314.

Johnson, Z. I., E. R. Zinser, A. Coe, N. P. McNulty, E. M. S. Woodward, and S. W. Chisholm. 2006. Niche partitioning among *Prochlorococcus* ecotypes along ocean-scale environmental gradients. Science **311:** 1737-1740.

Karl, D. M. and others 1995. Ecosystem Changes in the North Pacific Subtropical Gyre Attributed to the 1991-92 El-Nino. Nature **373:** 230-234.

Karl, D. M., and R. Lukas. 1996. The Hawaii Ocean Time-series (HOT) program: Background, rationale and field implementation. Deep-Sea Res. Part II-Top. Stud. Oceanogr. **43:** 129-156.

Kettler, G. C. and others 2007. Patterns and implications of gene gain and loss in the evolution of *Prochlorococcus*. Plos Genetics **3:** 2515-2528.

Legendre, P. and L. Legendre. 1998. Ecological Data Series. In: Numerical Ecology: Second English Addition. Elsevier Science B.V.: Amsterdam, pp 637-691.

Letelier, R. M. and others 2000. Role of late winter mesoscale events in the biogeochemical variability of the upper water column of the North Pacific Subtropical Gyre. Journal of Geophysical Research-Oceans **105:** 28723-28739.

Ludwig, W. and others 2004. ARB: a software environment for sequence data. Nucleic Acids Research **32:** 1363-1371.

Malmstrom, R. R., M. T. Cottrell, H. Elifantz, and D. L. Kirchman. 2005. Biomass production and dissolved organic matter assimilation by SAR11 bacteria in the Northwest Atlantic Ocean. Appl. Environ. Microbiol. **71:** 2979-2986.

Malmstrom, R. R., R. P. Kiene, M. T. Cottrell, and D. L. Kirchman. 2004. Contribution of SAR11 bacteria to dissolved dimethylsulfoniopropionate and amino acid uptake in the North Atlantic Ocean. Appl. Environ. Microbiol. **70:** 4129-4135.

Martiny, A. C., M. L. Coleman, and S. W. Chisholm. 2006. Phosphate acquisition genes in *Prochlorococcus* ecotypes: Evidence for genome-wide adaptation. Proceedings of the National Academy of Sciences of the United States of America **103:** 12552-12557.

Martiny, A. C., S. Kathuria, and P. M. Berube. 2009a. Widespread metabolic potential for nitrite and nitrate assimilation among *Prochlorococcus* ecotypes. Proceedings of the National Academy of Sciences of the United States of America **106:** 10787-10792.

Martiny, A. C., A. P. K. Tai, D. Veneziano, F. Primeau, and S. W. Chisholm. 2009b. Taxonomic resolution, ecotypes and the biogeography of *Prochlorococcus*. Environ. Microbiol. **11:** 823-832.

Michelou, V. K., M. T. Cottrell, and D. L. Kirchman. 2007. Light-stimulated bacterial production and amino acid assimilation by cyanobacteria and other microbes in the North Atlantic Ocean. Appl. Environ. Microbiol. **73:** 5539-5546.

Moore, L. R., and S. W. Chisholm. 1999. Photophysiology of the marine cyanobacterium *Prochlorococcus*: Ecotypic differences among cultured isolates. Limnol. Oceanogr. **44:** 628-638.

Moore, L. R., M. Ostrowski, D. J. Scanlan, K. Feren, and T. Sweetsir. 2005. Ecotypic variation in phosphorus acquisition mechanisms within marine picocyanobacteria. Aquat. Microb. Ecol. **39:** 257-269.

Moore, L. R., A. F. Post, G. Rocap, and S. W. Chisholm. 2002. Utilization of different nitrogen sources by the marine cyanobacteria *Prochlorococcus* and *Synechococcus*. Limnol. Oceanogr. **47:** 989-996.

Moore, L. R., G. Rocap, and S. W. Chisholm. 1998. Physiology and molecular phylogeny of coexisting *Prochlorococcus* ecotypes. Nature **393:** 464-467.

Morris, R. M. and others. 2002. SAR11 clade dominates ocean surface bacterioplankton communities. Nature **420:** 806-810.

Olson, R. J., S. W. Chisholm, E. R. Zettler, M. A. Altabet, and J. A. Dusenberry. 1990a. Spatial and Temporal Distributions of Prochlorophyte Picoplankton in the North-Atlantic Ocean. Deep-Sea Research Part a-Oceanographic Research Papers **37:** 1033-1051.

Olson, R. J., S. W. Chisholm, E. R. Zettler, and E. V. Armbrust. 1990b. Pigments, Size, and Distribution of Synechococcus in the North-Atlantic and Pacific Oceans. Limnol. Oceanogr. **35:** 45-58.

Osburne, M. and others. (2010). UV hyper-resistance in *Prochlorococcus* MED4 results from a single base pair deletion just upstream of an operon encoding nudix hydrolase and photolyase. Environ. Microbiol. (in press).

Partensky, F. and L. Garczarek. 2010. *Prochlorococcus*: Advantages and Limits of Minimalism. Annu. Rev. Marin. Sci, **Vol. 2:** 305-331.

Partensky, F., W. R. Hess, and D. Vaulot. 1999. *Prochlorococcus*, a marine photosynthetic prokaryote of global significance. Microbiology and Molecular Biology Reviews **63:** 106-+.

Promnares, K., J. Komenda, L. Bumba, J. Nebesarova, F. Vacha, and M. Tichy. 2006. Cyanobacterial small chlorophyll-binding protein ScpD (HliB) is located on the periphery of photosystem II in the vicinity of PsbH and CP47 subunits. Journal of Biological Chemistry **281:** 32705-32713.

Ramirez-Flandes, S., and O. Ulloa. 2008. Bosque: integrated phylogenetic analysis software. Bioinformatics **24:** 2539-2541.

Rocap, G., D. L. Distel, J. B. Waterbury, and S. W. Chisholm. 2002. Resolution of *Prochlorococcus* and *Synechococcus* ecotypes by using 16S-23S ribosomal DNA internal transcribed spacer sequences. Appl. Environ. Microbiol. **68:** 1180-1191.

Rocap, G. and others 2003. Genome divergence in two *Prochlorococcus* ecotypes reflects oceanic niche differentiation. Nature **424:** 1042-1047.

Sancar, G. B. 2000. Enzymatic photoreactivation: 50 years and counting. Mutation Research-Fundamental and Molecular Mechanisms of Mutagenesis **451:** 25-37.

Six, C., Finkel, Z.V., Irwin, A.J., and D.A. Campbell. 2009. Light variability illuminates niche-partitioning among marine picocyanobacteria. PLoS ONE **2(12):** e1341.

Stackebrandt, E. and B.M. Goebel. 1994. Taxonomic note: a place for DNA:DNA reassociation and 16S rRNA sequence analysis in the present species definition in bacteriology. Int. J. Syst. Bacteriol. **44:** 846-849.

Steinberg, D. K., C. A. Carlson, N. R. Bates, R. J. Johnson, A. F. Michaels, and A. H. Knap. 2001. Overview of the US JGOFS Bermuda Atlantic Time-series Study (BATS): a decade-scale look at ocean biology and biogeochemistry. Deep-Sea Res. Part II-Top. Stud. Oceanogr. **48:** 1405-1447.

Treusch, A. H. and others 2009. Seasonality and vertical structure of microbial communities in an ocean gyre. Isme Journal **3:** 1148-1163.

Turesson, G. 1922. Species and the variety as ecological units. Hereditas **3:** 100-113.

Venter, J. C. and others 2004. Environmental genome shotgun sequencing of the Sargasso Sea. Science **304:** 66-74.

Vila-Costa, M., R. Simo, H. Harada, J. M. Gasol, D. Slezak, and R. P. Kiene. 2006. Dimethylsulfoniopropionate uptake by marine phytoplankton. Science **314:** 652-654.

Ward, D.M. and others. 2006. Cyanobacterial ecotypes in the microbial mat community of Mushroom Spring (Yellowstone National Park, Wyoming) as species-like units linking microbial community composition, structure and function. Philos. Trans. R. Soc. London (Biol). **361:1475** 1997-2008.

West, N. J., and D. J. Scanlan. 1999. Niche-partitioning of *Prochlorococcus* populations in a stratified water column in the eastern North Atlantic Ocean. Appl. Environ. Microbiol. **65:** 2585-2591.

West, N. J. and others 2001. Closely related *Prochlorococcus* genotypes show remarkably different depth distributions in two oceanic regions as revealed by in situ hybridization using 16S rRNA-targeted oligonucleotides. Microbiology **147:** 1731-1744.

White, A. E., Y. H. Spitz, and R. M. Letelier. 2007. What factors are driving summer phytoplankton blooms in the North Pacific Subtropical Gyre? Journal of Geophysical Research-Oceans **112**.

Wu, J. F., W. Sunda, E. A. Boyle, and D. M. Karl. 2000. Phosphate depletion in the western North Atlantic Ocean. Science **289:** 759-762.

Yao, D. and others 2007. Localization of the small CAB-like proteins in photosystem II. Journal of Biological Chemistry **282:** 267-276.

Zinser, E. R. and others 2006. *Prochlorococcus* ecotype abundances in the North Atlantic Ocean as revealed by an improved quantitative PCR method. Appl. Environ. Microbiol. **72:** 723-732.

Zinser, E. R., Z. I. Johnson, A. Coe, E. Karaca, D. Veneziano, and S. W. Chisholm. 2007. Influence of light and temperature on *Prochlorococcus* ecotype distributions in the Atlantic Ocean. Limnol. Oceanogr. **52:** 2205-2220.

Zubkov, M. V., B. M. Fuchs, G. A. Tarran, P. H. Burkill, and R. Amann. 2003. High rate of uptake of organic nitrogen compounds by *Prochlorococcus* cyanobacteria as a key to their dominance in oligotrophic oceanic waters. Appl. Environ. Microbiol. **69:** 1299-1304.

Zwirglmaier, K., J. L. Heywood, K. Chamberlain, E. M. S. Woodward, M. V. Zubkov, and D. J. Scanlan. 2007. Basin-scale distribution patters of picocyanobacterial lineages in the Atlantic Ocean. Environ. Microbiol. **9:** 1278-1290.

Figure Legends

Figure 1: Ecotype distribution patterns in relation to depth and photosynthetically active radiation. A smoothed illustration of relationship between ecotype abundance and irradiance, calculated from a compilation of data from all 5 years, was plotted for HOT (A) and BATS (C). Data were smoothed by locally weighted regression of ecotype abundance against irradiance. Note, smoothed data exclude profiles with a mixed layer depth >100m. Representative depth profiles of ecotype abundance at HOT (B,E) and BATS (D,F) during periods of stratification and deep mixing. Dashed lines mark the mixed layer depth, and error bars represent one standard deviation. An illustration of the color scheme and general phylogenetic relationships among ecotypes (after Kettler et al. 2007; Rocap et al. 2002) is displayed in panel G. This tree serves only as reference to the other panels; branch lengths are not to scale.

Figure 2: Abundance of *Prochlorococcus* and *Synechococcus* at BATS and HOT determined by flow cytometry (bottom x-axis). Abundance levels from this study are compared with those collected at BATS from 1990-1994 (DuRand et al. 2001) (A,B), and at HOT from 1991-1995 (C,D) (top x-axis), which were also determined by flow cytometry.

Figure 3: Integrated ecotype abundance (0-200m) at BATS (A) and HOT (B) from 2003-2008. Solid lines represent abundances smoothed by locally weighted regression for eMIT9312 (yellow), eMED4 (green), eNATL (blue), eSS120 (purple), and eMIT9313 (red).

Figure 4: Ecotype abundance at BATS (A-E) and HOT (F-J) from 2003-2008. Sampling depths at HOT and BATS are indicated by the points overlaying panels A and F. The solid lines indicate the mixed layer depth.

Figure 5: Integrated ecotype abundance of in different regions of the euphotic zone at BATS (A-E) and HOT (F-J). The regions from 0-60m, 60-120m, and 120m are identified by filled squares, open circles, and open triangles, respectively. Abundance was smoothed using locally weighted regression to eliminate low frequency variation.

Figure 6: Response of *Prochlorococcus* strains MED4, NATL2a, and SS120 to light-shock. *In vivo* chlorophyll fluorescence of duplicate cultures acclimated to 35 µE m^{-2} s^{-1}, exposed to 400 µE m^{-2} s^{-1} for four hours (grey area), and returned to 35 µE m^{-2} s^{-1}. Controls did not experience light shock. Error bars represent one standard deviation.

Supplementary Figure 1: Neighbor-joining tree of ITS sequences amplified from both HOT and BATS using re-designed qPCR primers specific for eSS120 ecotype. Amplified ITS sequences are identified by name "HOT_BATS." Previously sequenced genomes are marked with an *. Bootstrap values >40 are indicated (n=100).

Supplementary Figure 2: Ecotype abundance vs. photosynthetically-active radiation at BATS (A-E) and HOT (F-J). Data point colors indicate temperature. Black lines represent a locally weighted regression of the relationship between abundance and

irradiance. No profiles were excluded based on mixed layer depth (compare with Fig. 1a,b).

Supplementary Figure 3: Spectral analysis of integrated (0-200m) ecotype abundance at BATS. Peaks represent unbiased power spectral density at periods of 1 month.

Supplementary Figure 4: Autocorrelation of integrated abundance at BATS with lags of one month. Dashed lines represent two standard deviations around a correlation coefficient of 0.

Supplementary Figure 5: Spectral analysis of integrated (0-200m) ecotype abundance at HOT. Peaks represent unbiased power spectral density at periods of 1 month.

Supplementary Figure 6: Autocorrelation of integrated abundance at HOT with lags of one month. Dashed lines represent two standard deviations around a correlation coefficient of 0.

Supplementary Figure 7: Annual pattern of integrated abundance, surface temperature, surface light levels, and mixed layer depth at BATS. Data represent a smoothed compilation of all five years.

Supplementary Figure 8: Response of *Prochlorococcus* strains MED4, NATL2a, and SS120 to light-shock. Cell counts determined by flow cytometry of duplicate cultures

acclimated to 35 µE m^{-2} s^{-1}, exposed to 400 µE m^{-2} s^{-1} for four hours (grey area), and returned to 35 µE m^{-2} s^{-1}. Controls did not experience light shock. Error bars represent one standard deviation.

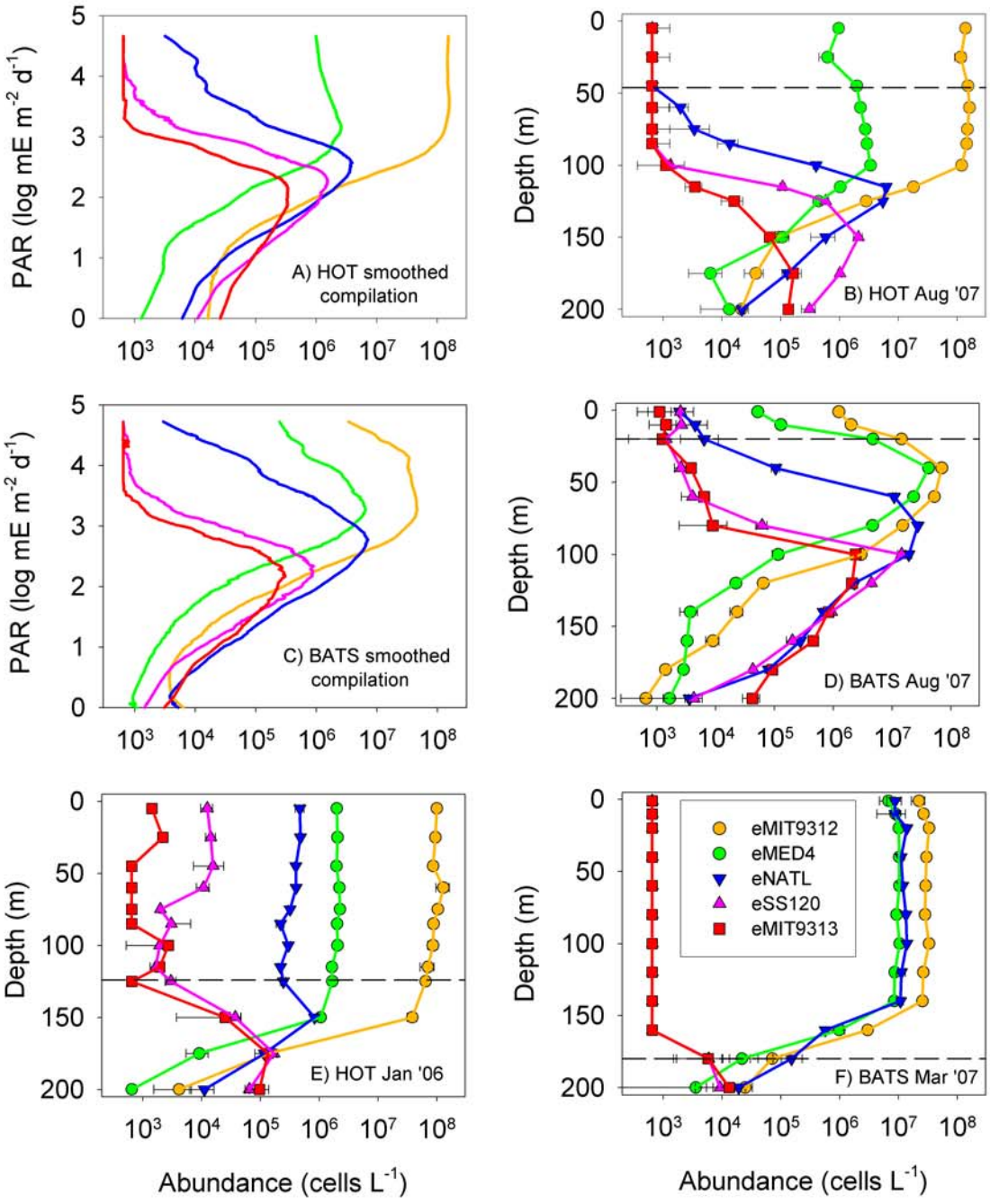
PAR (log mE m-2 d-1)
A) HOT smoothed compilation
B) HOT Aug '07
C) BATS smoothed compilation
D) BATS Aug '07
E) HOT Jan '06
F) BATS Mar '07
Depth (m)
Abundance (cells L-1)
eMIT9312
eMED4
eNATL
eSS120
eMIT9313

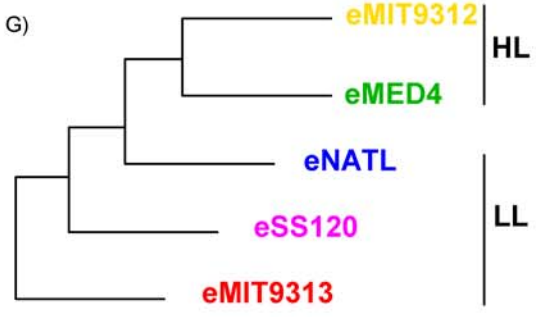
G)
eMIT9312
eMED4
eNATL
eSS120
eMIT9313
HL
LL

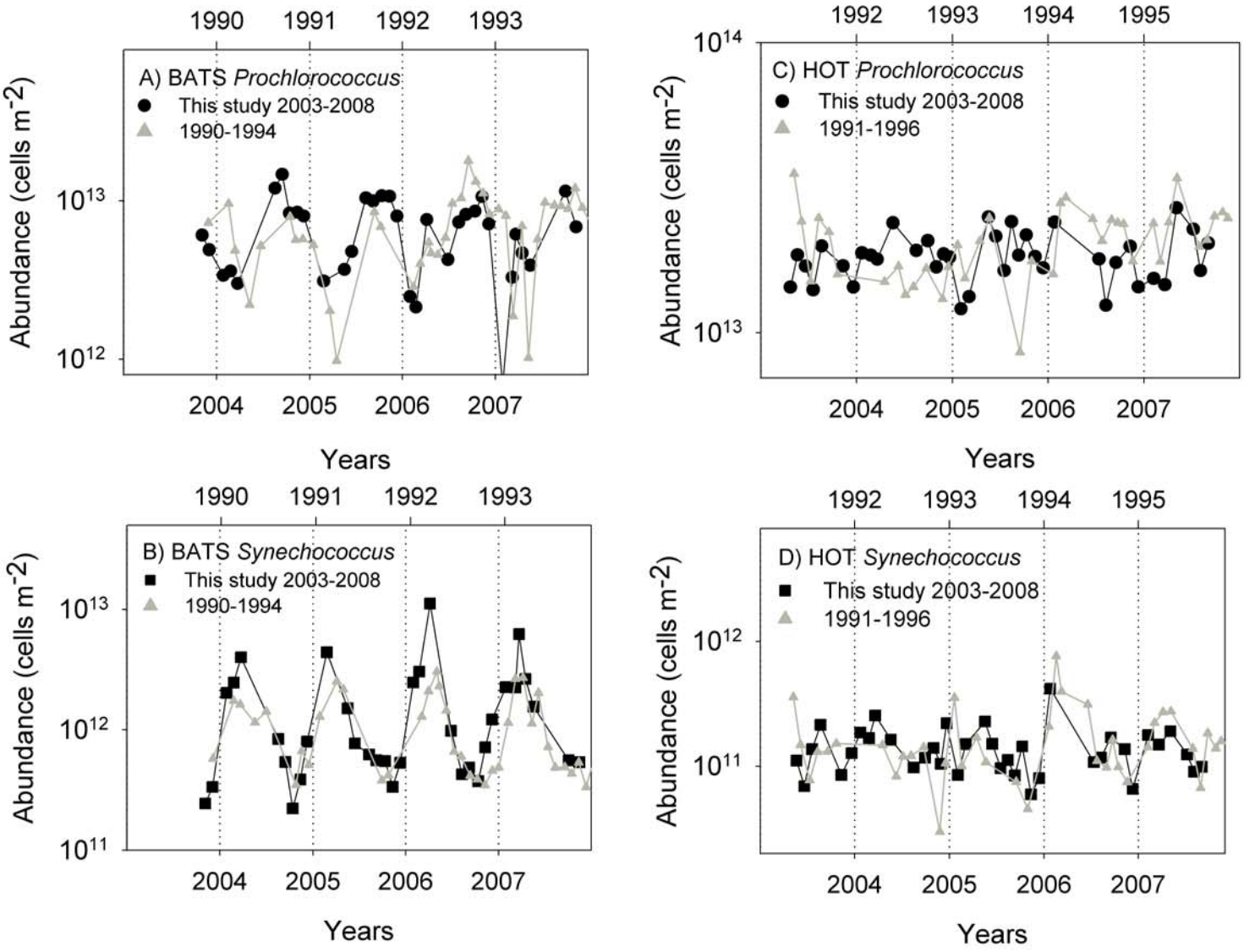
A) BATS Prochlorococcus
This study 2003-2008
1990-1994
B) BATS Synechococcus
This study 2003-2008
1990-1994
C) HOT Prochlorococcus
This study 2003-2008
1991-1996
D) HOT Synechococcus
This study 2003-2008
1991-1996
Abundance (cells m-2)
Years
1990
1991
1992
1993
1994
1995
2004
2005
2006
2007
10^11
10^12
10^13
10^14

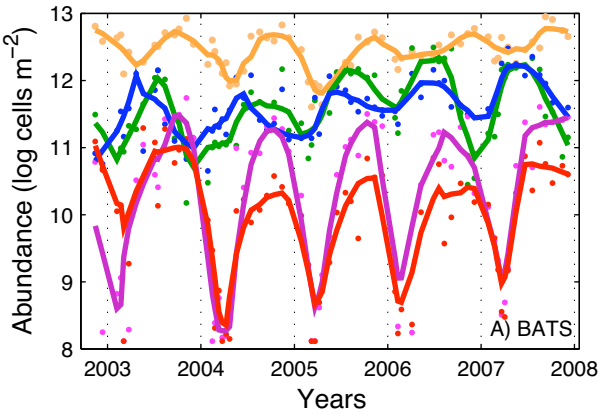
Abundance (log cells m^{-2})
13
12
11
10
9
8
2003
2004
2005
2006
2007
2008
Years
A) BATS

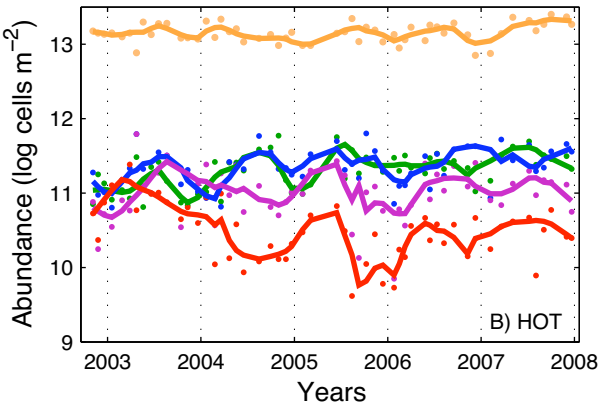
Abundance (log cells m^{-2})
13
12
11
10
9
2003
2004
2005
2006
2007
2008
Years
B) HOT

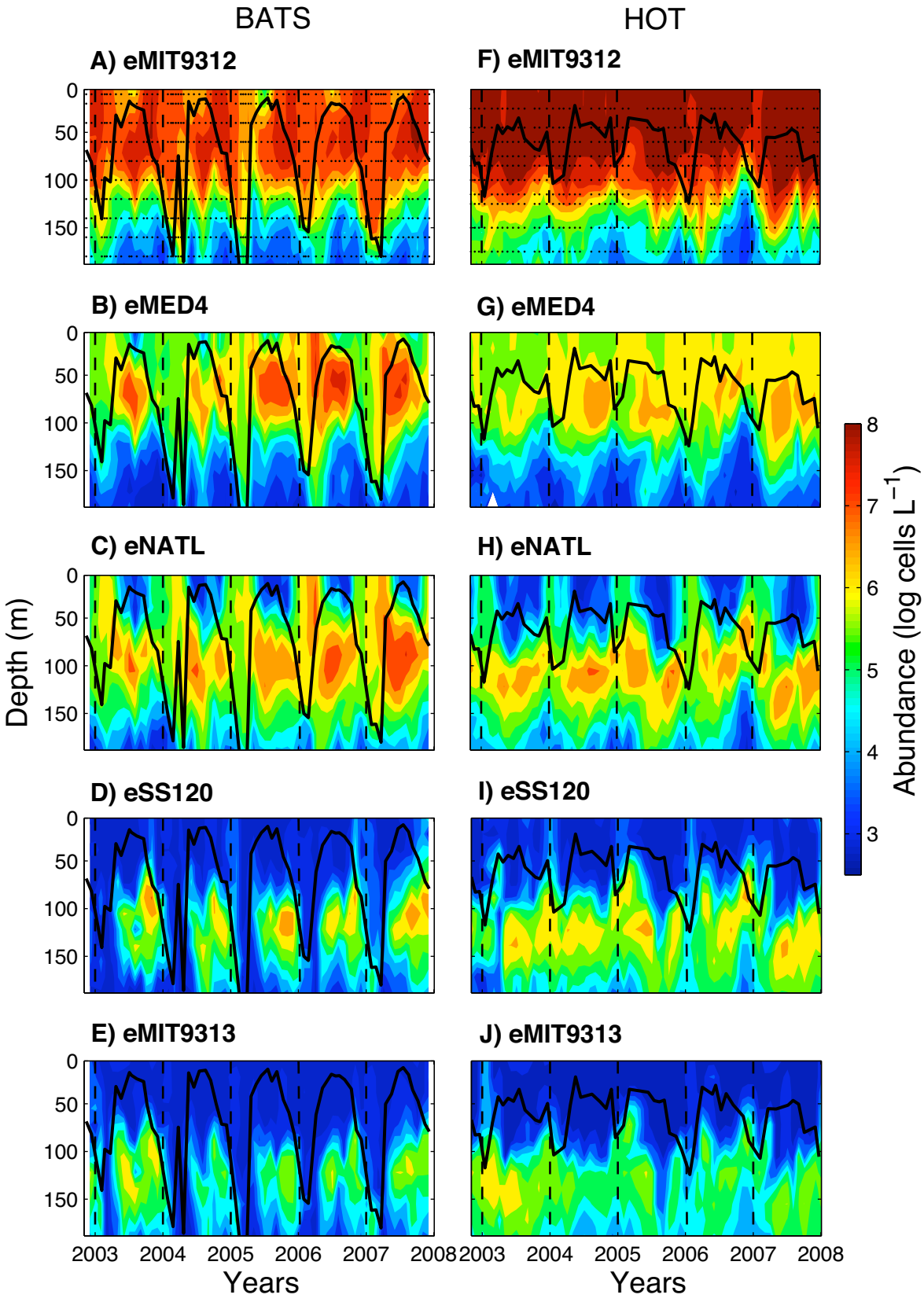
BATS
HOT
A) eMIT9312
F) eMIT9312
B) eMED4
G) eMED4
C) eNATL
H) eNATL
D) eSS120
I) eSS120
E) eMIT9313
J) eMIT9313
Depth (m)
0
50
100
150
2003
2004
2005
2006
2007
2008
Years
Abundance (log cells L^{-1})
3
4
5
6
7
8

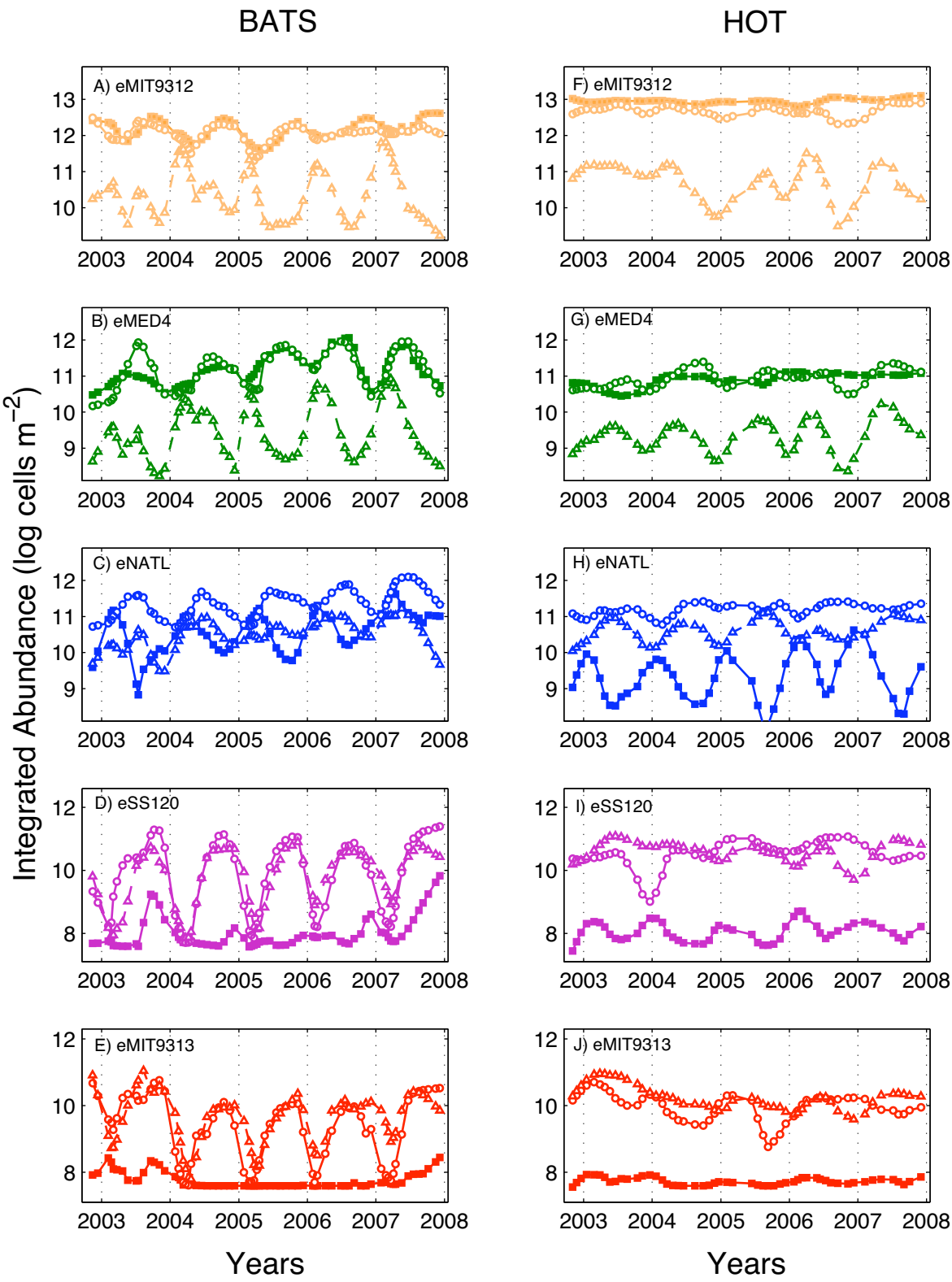
BATS
HOT
A) eMIT9312
F) eMIT9312
B) eMED4
G) eMED4
C) eNATL
H) eNATL
D) eSS120
I) eSS120
E) eMIT9313
J) eMIT9313
Integrated Abundance (log cells m^{-2})
Years
Years

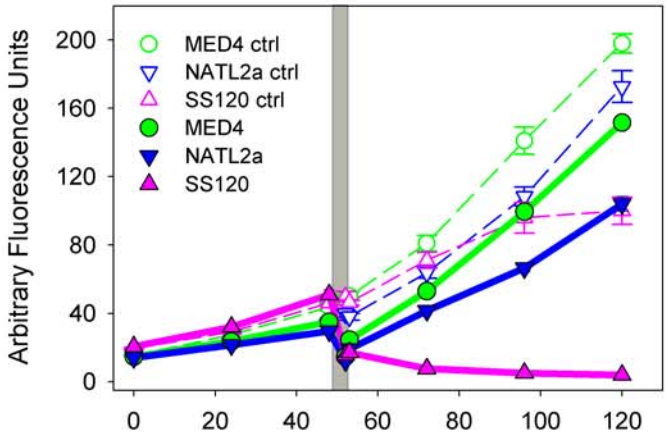
Arbitrary Fluorescence Units
200
160
120
80
40
0
0
20
40
60
80
100
120
MED4 ctrl
NATL2a ctrl
SS120 ctrl
MED4
NATL2a
SS120

Table 1: Average depth of maximum ecotype abundance at HOT and BATS (mean ± STD). Samples collected when the mixed layer depth was >100m were excluded. Values with different superscripts are significanlty different (Tukey post test of repeated measures ANOVA; alpha = 0.05).

Ecotype	HOT (m)	BATS (m)
eMIT9312	42 ± 27^{A}	54 ± 28^{A}
eMED4	71 ± 29^{B}	60 ± 26^{A}
eNATL	105 ± 18^{C}	87 ± 22^{B}
eSS120	118 ± 26^{D}	101 ± 28^{C}
eMIT9313	128 ± 30^{D}	107 ± 25^{C}

Table 2: Correlation and cross-correlation between integrated ecotype abundance (0-200m) and mixed layer depth at BATS. The coefficient of cross-correlation represents the relationship between abundance at one month and the mixed layer depth from previous months. The maximum positive cross-correlation is reported along with the delay in months (lag) between abundance and mixed layer depth when correlation is greatest. * indicates $p<0.05$.

Ecotype	Correlation coeff. (lag in months)	Max. cross-correlation coeff. (lag in months)
eMIT9312	-0.06 (0)	0.61* (8)
eMED4	-0.62* (0)	0.58* (5)
eNATL	-0.54* (0)	0.65* (4)
eSS120	-0.60* (0)	0.66* (8)
eMIT9313	-0.46* (0)	0.61* (8)

Supplementary Figure 1

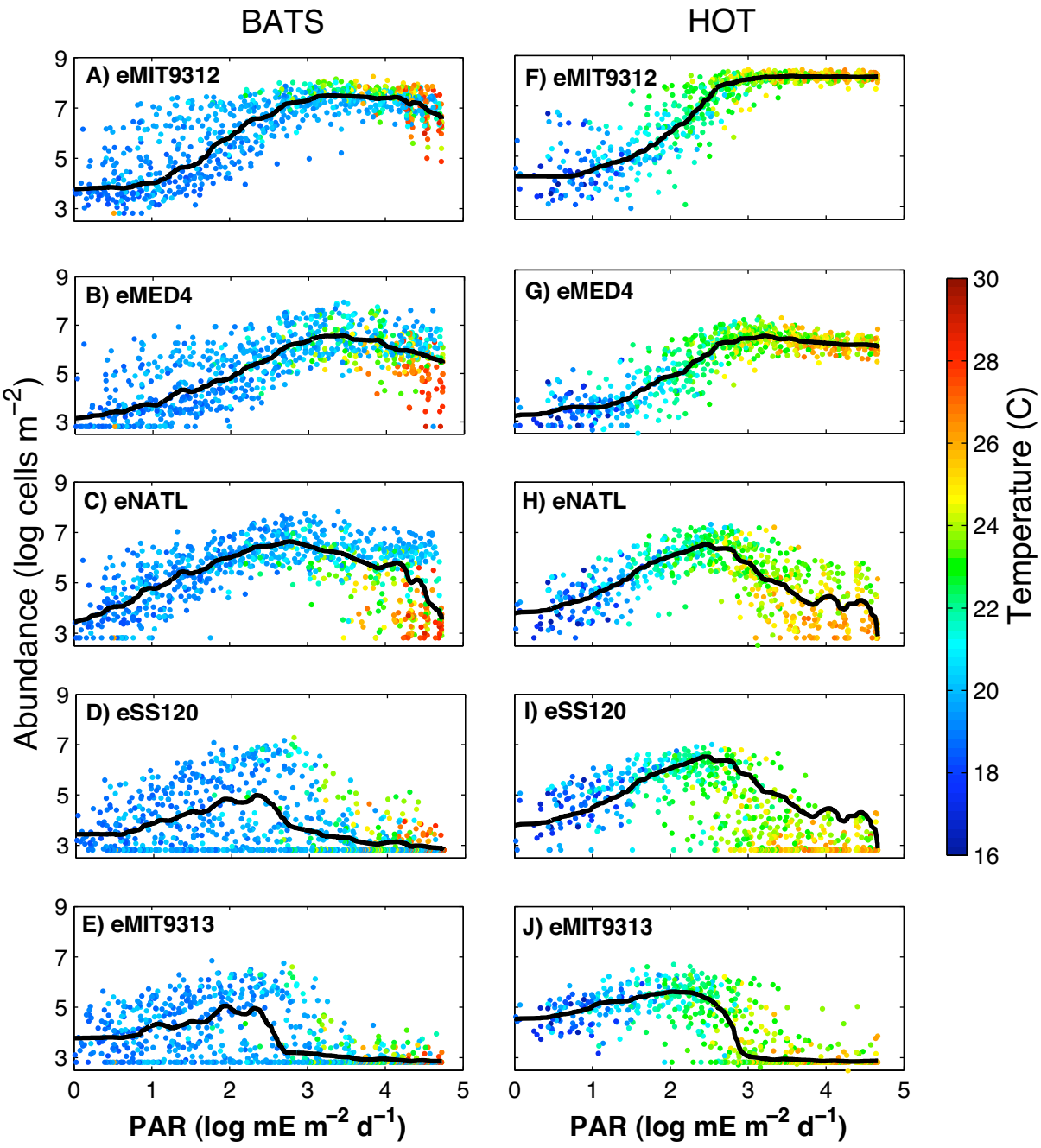
BATS
HOT
A) eMIT9312
F) eMIT9312
B) eMED4
G) eMED4
C) eNATL
H) eNATL
D) eSS120
I) eSS120
E) eMIT9313
J) eMIT9313
Abundance (log cells m^{-2})
PAR (log mE m^{-2} d^{-1})
PAR (log mE m^{-2} d^{-1})
Temperature (C)
3
5
7
9
0
1
2
3
4
5
16
18
20
22
24
26
28
30

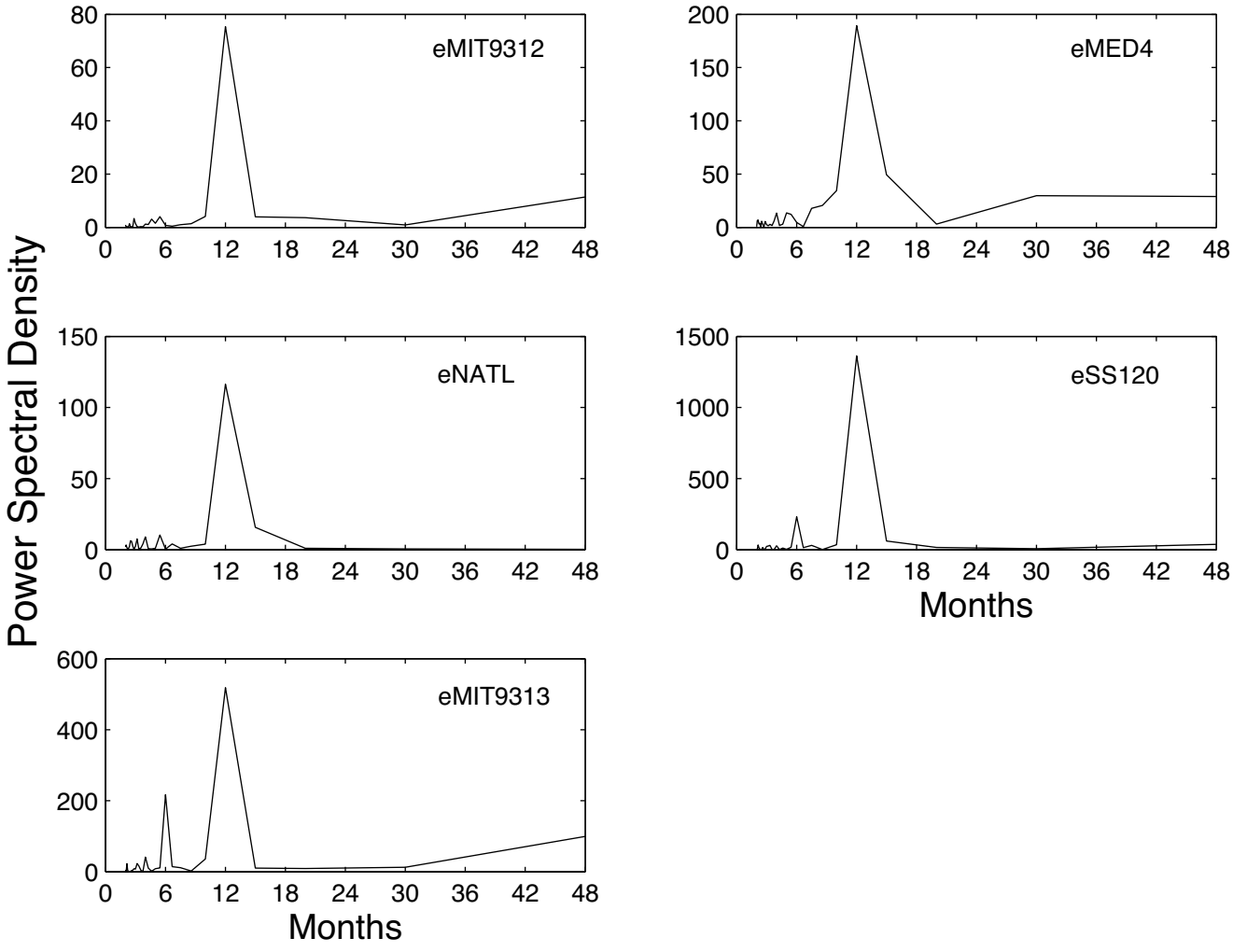
Power Spectral Density
eMIT9312
eMED4
eNATL
eSS120
eMIT9313
Months
Months

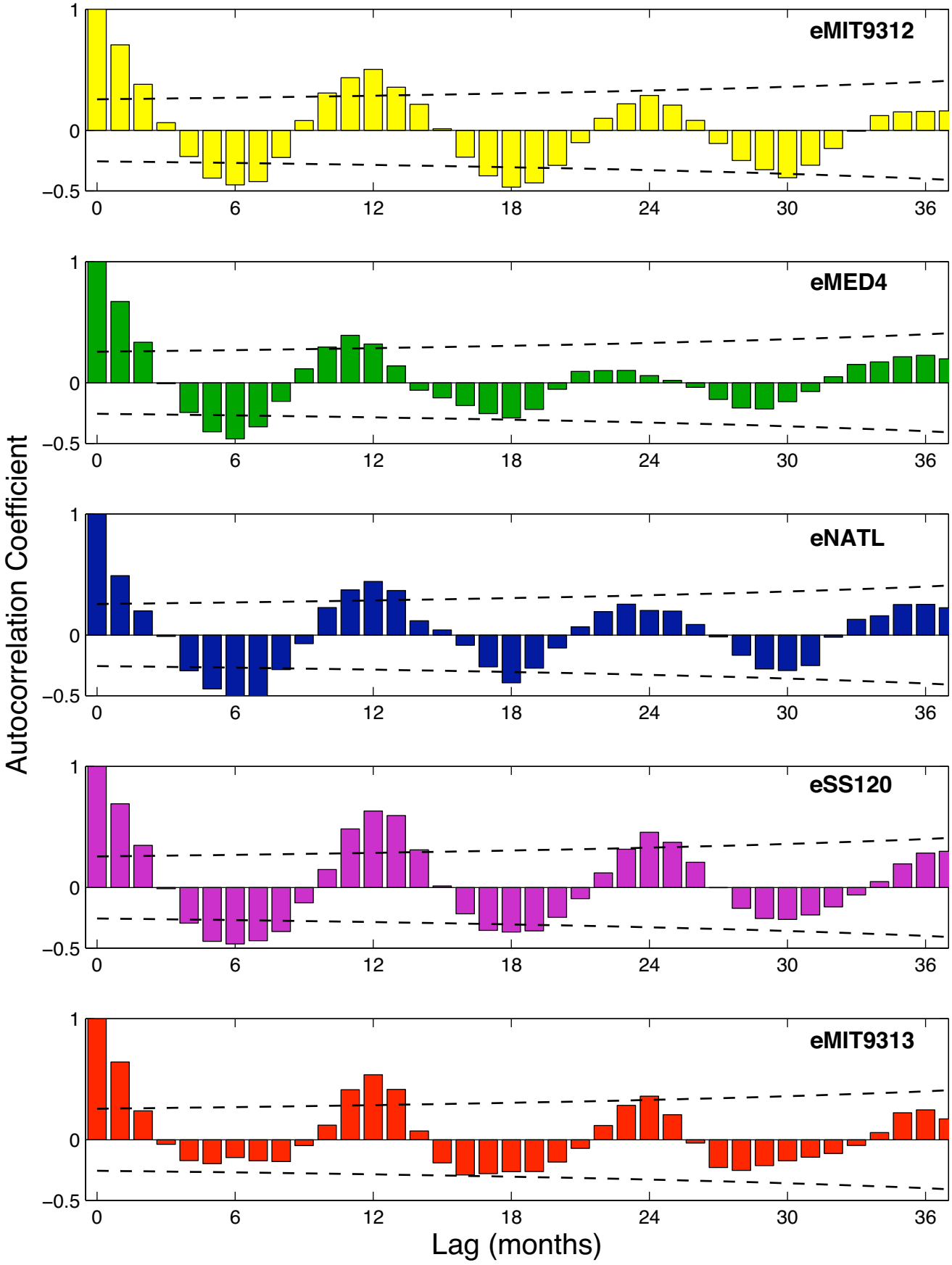
eMIT9312
eMED4
eNATL
eSS120
eMIT9313
Autocorrelation Coefficient
Lag (months)
1
0
−0.5
0
6
12
18
24
30
36

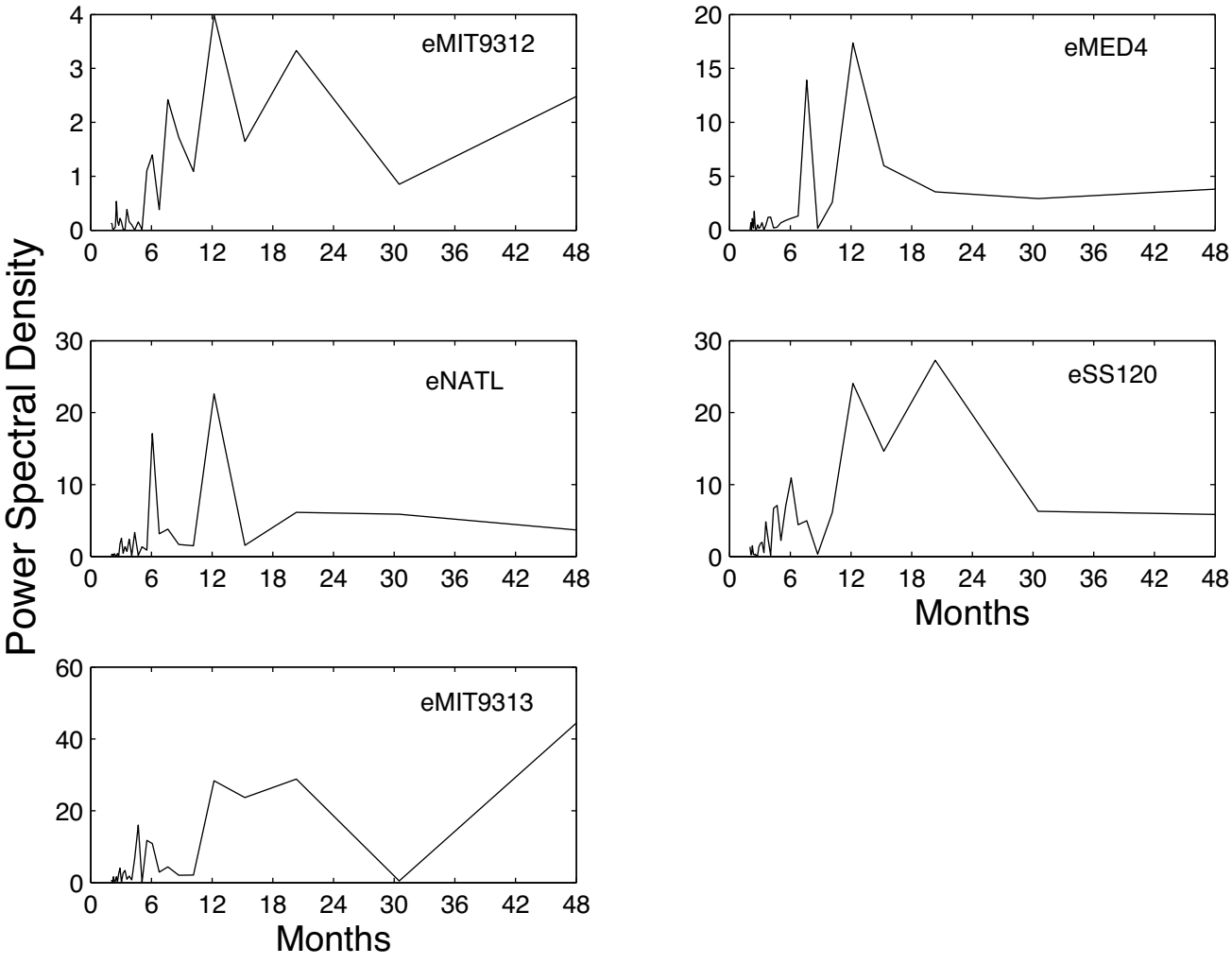
Power Spectral Density
eMIT9312
eMED4
eNATL
eSS120
eMIT9313
Months
Months

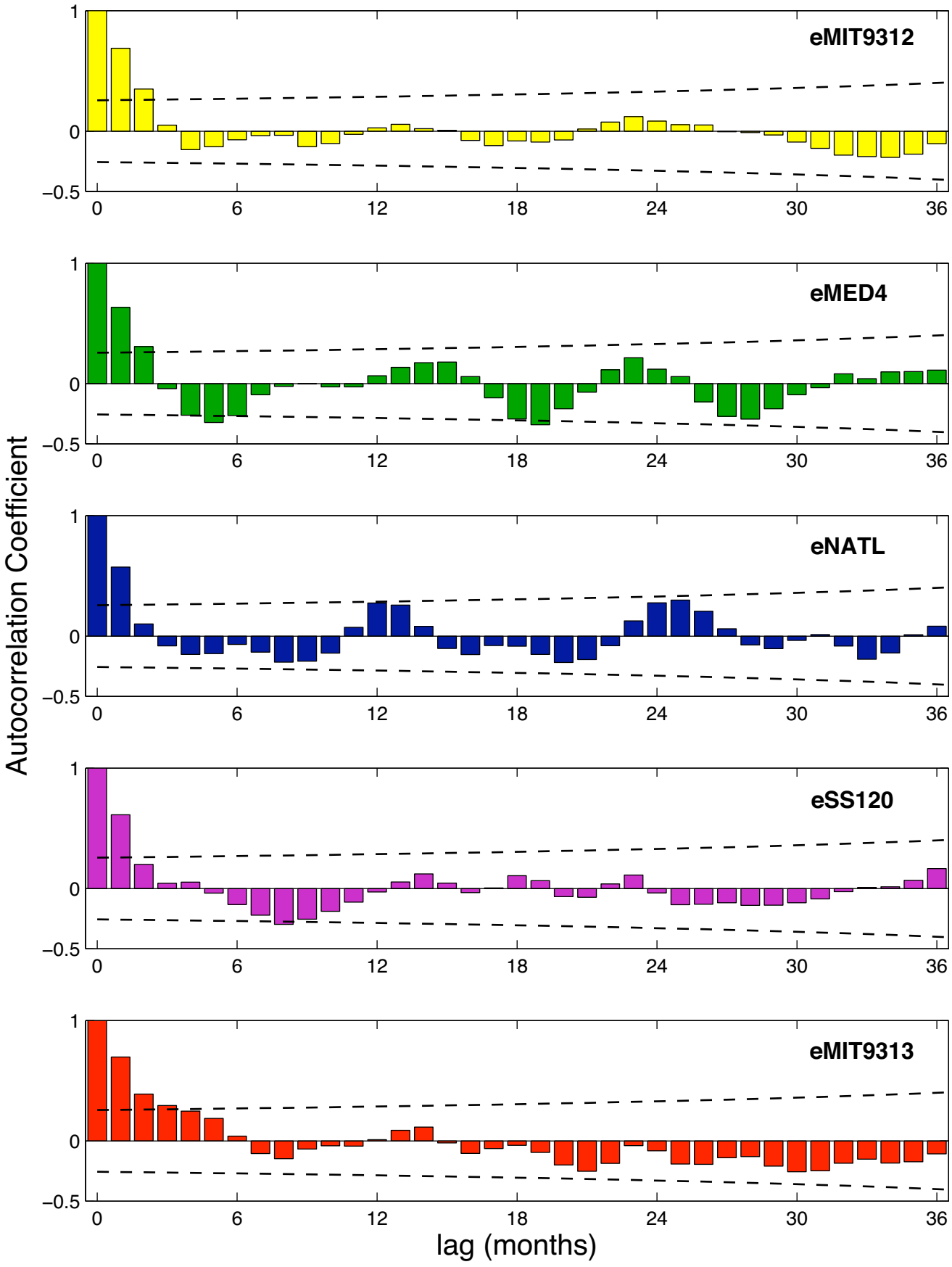
eMIT9312
eMED4
eNATL
eSS120
eMIT9313
Autocorrelation Coefficient
lag (months)
1
0
−0.5
0
6
12
18
24
30
36

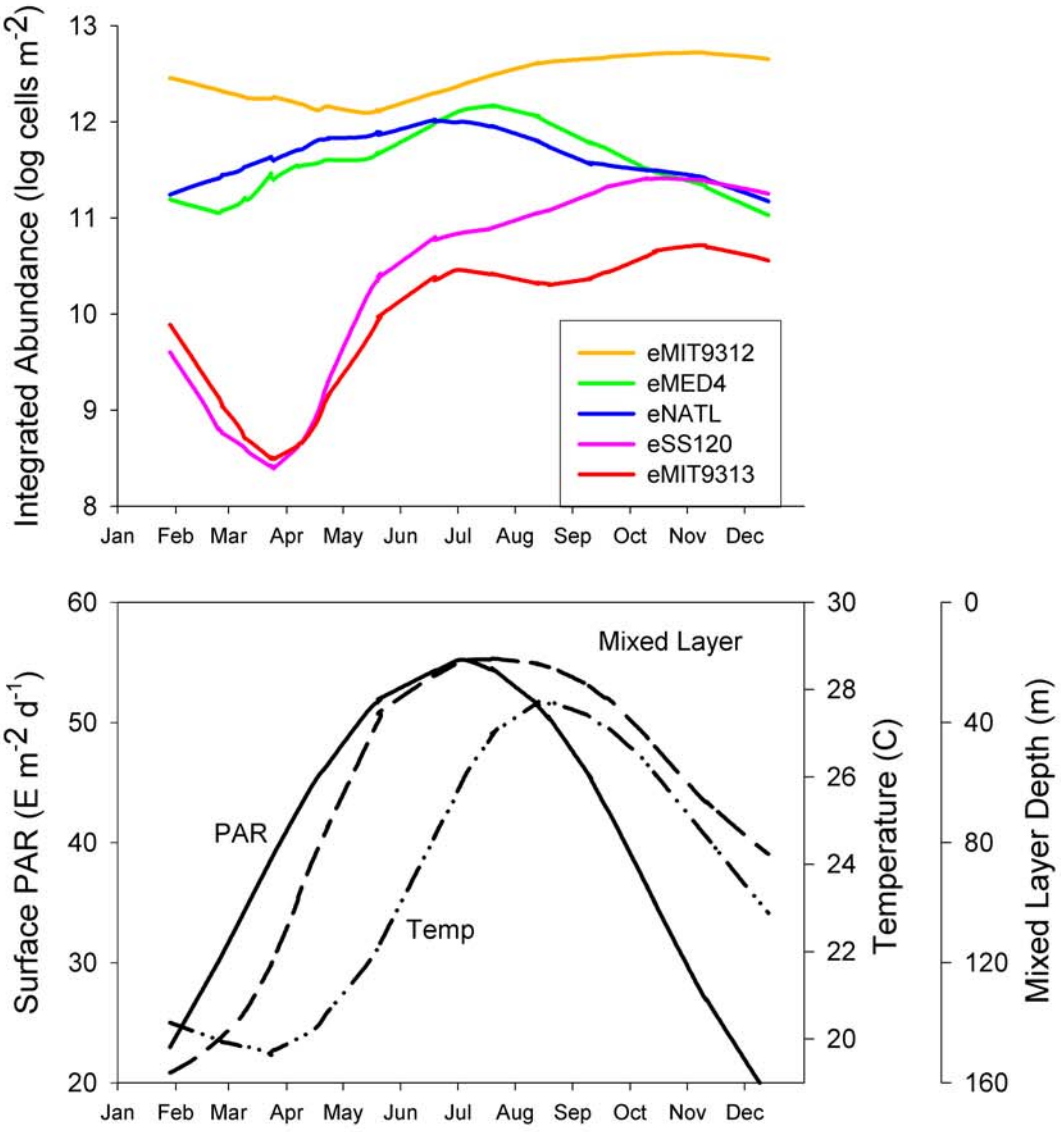
Integrated Abundance (log cells m-2)
13
12
11
10
9
8
Jan Feb Mar Apr May Jun Jul Aug Sep Oct Nov Dec
eMIT9312
eMED4
eNATL
eSS120
eMIT9313
Surface PAR (E m-2 d-1)
60
50
40
30
20
Mixed Layer
PAR
Temp
30
28
26
24
22
20
Temperature (C)
0
40
80
120
160
Mixed Layer Depth (m)

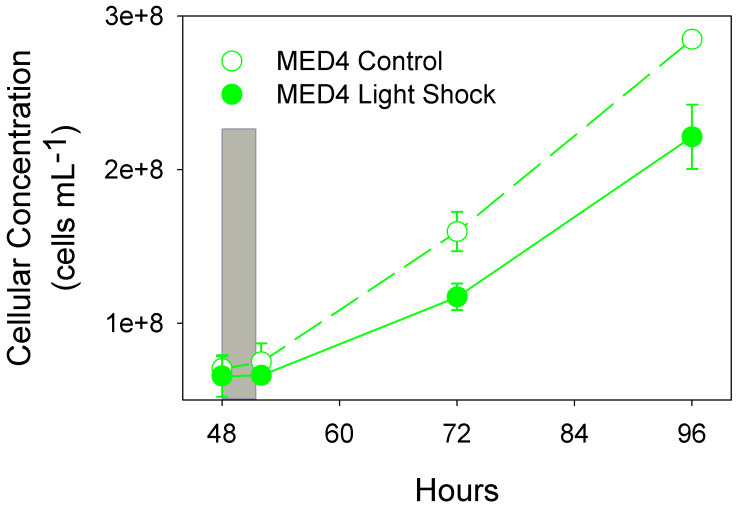
3e+8
2e+8
1e+8
Cellular Concentration
(cells mL-1)
MED4 Control
MED4 Light Shock
48
60
72
84
96
Hours

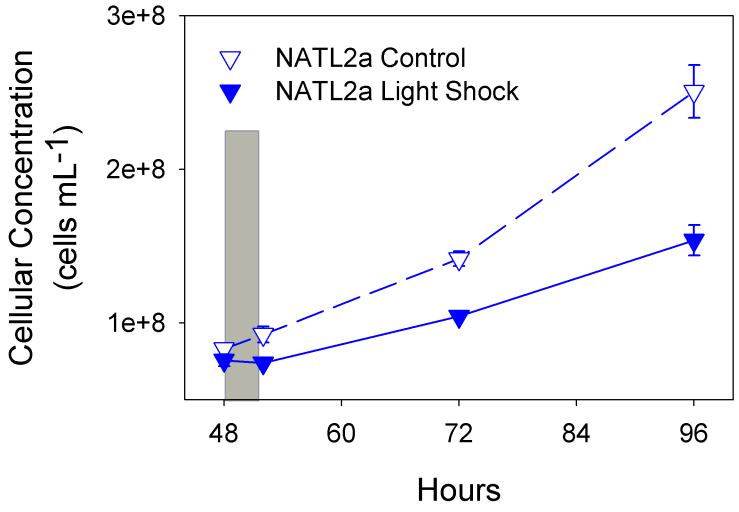
3e+8
2e+8
1e+8
Cellular Concentration
(cells mL-1)
NATL2a Control
NATL2a Light Shock
48
60
72
84
96
Hours

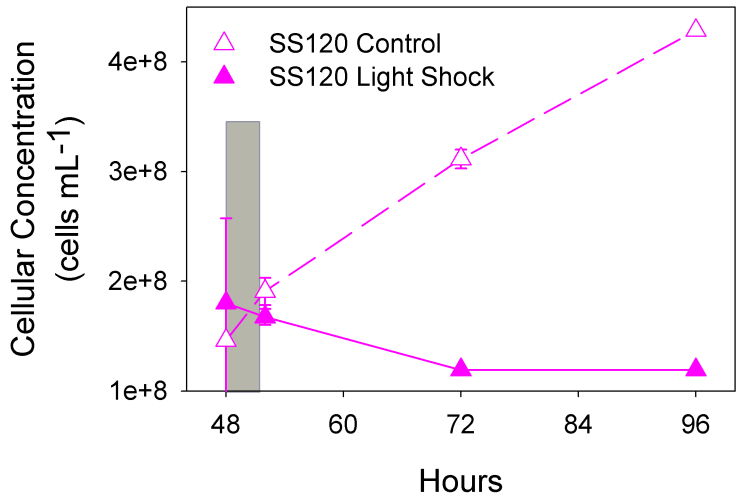
4e+8
3e+8
2e+8
1e+8
Cellular Concentration
(cells mL-1)
SS120 Control
SS120 Light Shock
48
60
72
84
96
Hours